Bulletin of Geosciences, Vol. 79, No. 4, 251–268, 2004

Water-related defects in quartz

Nina G. Stenina

Institute of Geology SBRAS, Koptyug av. 3, Novosibirsk-90, 630090, Russia. E-mail: stenina@yandex.ru

Abstract. The mode of incorporation of water and trace elements into silica matrices was studied in natural quartz of various origins: hydrothermal, magmatic, pegmatitic, and generations of vein quartz related to ore mineralization. Several methods were used toward identifying different manifestations of water-trace element defects. Transmission electron microscopy (TEM), as a unique direct tool for the imaging and identification of lattice defects, played an important role. IRS, TG, chemical analysis (AAS), X-ray microprobe, X-ray powder diffraction, and EPR were used for obtaining additional information on the nature of the complex defects. As a result, we propose a model for the combined silica-water-trace element defect [$2SiO_3$ □ - OH_2 – $M^{n+}2M^{m+}O'_4$] (where □ is a vacancy, O' is O and other volatiles such as S, Cl, etc.), called an aqua-complex. Aqua-complexes are units of the mineral-forming medium. Quartz (SiO_2), which corresponds to the left part of aqua-complex, is crystallized as a result of disintegration of the whole species. Non-disintegrated aqua-complexes become trapped during the formation of quartz. Single aqua-complexes are crystallographically accommodated into the SiO_4 framework, whereas their unordered segregations, which are actually micro-portions of the mineral-forming medium, are incorporated into the silica bulk as glass-like inclusions ("gel-defects"). Aqua-complexes are metastable species in quartz. During post-crystallization cooling of the mineral they may disintegrate into water-containing bubbles saturated with basic radicals, and acidic and volatile elements. As the thermodynamic parameters in the mineral system change, the aqua-complex constituents H (H_2O) and foreign cations M^{n+} and M^{m+} migrate through the SiO_4-lattice, which also becomes rearranged in this process. Such properties of the aqua-complex explain the elusive character of water-related defects in quartz.

Key words: natural quartz, water speciation, transmission electron microscopy, aqua-complex

Introduction

Water is a constant impurity in most silica varieties, actively participating in mineral and rock transformations. Investigations throughout the past 50 years have shown that water plays a leading role in the generation of various silica modifications. As a result, abundant experimental data on the incorporation of H_2O and trace elements in quartz has been obtained. Nevertheless, principal questions concerning the origins of water in silica minerals and water speciation in quartz have not yet been adequately answered. However, these issues are of fundamental importance, as the water incorporated into silicate matter exerts a tremendous effect on the mechanism and kinetics of mineral transformations and on the deformation behaviour of rocks.

The content of water in crystalline forms of silica is much lower than in cryptocrystalline and amorphous varieties, some hundreds ppm, and up to 6–8wt%, respectively. Among these forms, α-quartz is the most common form under the P-T conditions existing in the Earth's crust. It should be expected that a low (in comparison with other silica forms) content of water in quartz would allow us to study the "anatomy" of water speciation in silica matter and to answer the following principal questions: (1) Which species (H_2O, OH^-, Si — OH, H^+ or H_3O^+) is the most adequate form of water defect in silica matrices? (2) Are they point defects or their associations? (3) What is the relation, if any, between H-defects and trace elements in the quartz matrix? (4) Do H-defects represent disturbances of regular structure, or are they incorporated in any some way into the unordered lattice? (5) Is there any relation between the free water included in the bubbles and the structural water? (6) What is the significance of the correlation between the mode of water incorporation into a silica matrix, the total water content, and the modifications of silica minerals? A final question derived from the forgoing would be: (7) Is there any universal water-related defect that could explain all manifestations of H_2O and trace elements in quartz?

In this paper, a model for a combined water-trace element defect in quartz, called an aqua-complex, is presented. The proposed view of the H-defect is based on data from natural quartz samples obtained by TEM in combination with other methods.

Review of water and trace element speciation in silica minerals

Amorphous (glass-like, opaline) and micro-crystalline (chalcedony, agate, etc.) silica minerals, and many forms of natural and synthetic quartz have been studied by various instrumental methods (Scholze 1959a, b, 1960, Langer and Flörke 1974a, b, Flörke et al. 1982, Frondel 1982, Graetsch et al. 1985, Heaney 1993, Hopkinson et al. 1999). Infrared spectroscopy (IRS) is widely recognized as the most suitable tool for detecting the water content in silicates and determining its speciation. Transmission electron microscopy (TEM), cathodoluminescence (CL), X-ray, and other methods are also used for obtaining more information on the nature of H-defects.

Despite the abundance of studied silica minerals and the diversity of methods used in their investigation, no universally accepted view of the nature of invariant SiO_2 – H_2O partnership as arisen, and the classification of H-defects in silica has been rather conventional. The major problem concerning the state of water in silica minerals is whether it

is bound to the silica matrix or not. The shift of the characteristic H_2O band centred around 3400 cm^{-1} to the ice band at 3200 cm^{-1} in the IR-spectra at 78 °C is an unambiguous criterion of the availability of free or physical water. It is accepted that H_2O molecules are contained in gas-liquid inclusions and are adsorbed onto the walls of microfractures within the quartz bulk. This form of water is most typical of the natural "milky" quartz; it also arises in synthetic quartz samples after being heated above 500 °C. Thus, the presence of physical water is readily detectible.

Another form of water present in silica matrices is the structurally bound, or crystallochemical water. This is the water incorporated into the SiO_4-framework, and forms chemical bonds with the host matrix. The above-mentioned questions about H-defects are related mainly to this form of water. In the IR-spectra, all ranges are informative in the investigation of structurally bound water, as they fix its various manifestations. The range 3000–3600 cm^{-1} encompasses the fundamental OH-stretching vibrations of H_2O molecules. The fundamental research by Bambauer et al. (1961), Brunner et al. (1961), and Kats (1962), as well as many of their followers, has contributed much to the identification of the bands inhabiting this range. There are two distinct kinds of absorption within this range: numerous sharp pleochroic peaks, and a broad isotropic band centred at about 3400 cm^{-1} that does not sharpen into the ice band at low temperatures.

According to Frondel (1982), the first quartz is "quartz A" and second is "quartz B". Sharp and broad bands within this range are correspondingly assigned to OH in the well-defined structural sites (i.e. in the regular silica lattice), and to hydroxyl groups incorporated into the unordered glass- or opal-like micro areas, termed firstly by Brunner et al. (1961) as "gel-like" defects. Sharp pleochroic peaks are typical of natural clear quartz varieties with minor amounts of water. Broad isotropic absorption bands are characteristic of wet synthetic quartz; they occur in the spectra of some coloured samples such as lamellar-twinned amethyst (Brunner et al. 1961, Kekulawala et al. 1978), and in amethyst-citrine (Balitskii and Balitskaya 1985).

The NIR range (4000–7000 cm^{-1}) can provide information toward answering the following questions: (1) Is OH incorporated into the silica lattice as an independent species or is it a constituent of an H_2O molecule? (2) Are hydroxyl groups bound in some way with the silica environment? Two characteristic bands (4500 cm^{-1} and 5200 cm^{-1}) were examined in detail in water-containing silica (quartz, glass, crystalline and opaline varieties) in order to answer these questions. Scholze (1959a, b, 1960) and Brunner et al. (1961) showed that the combination band ($\nu_2 + \nu_3$) at 5200 cm^{-1} must be attributed to H_2O molecules, and that the combination band ($\nu_{OH} + \delta_{SiOH}$) at 4500 cm^{-1} to OH-groups bound within the SiO_4 – framework (i.e. to the Si — OH silanol groups).

The fine structure of these bands expressed in the splitting at 5200 → 5260 cm^{-1} and 5100 cm^{-1}, 4500 cm^{-1} → 4500 cm^{-1} and 4420 cm^{-1} in hyalite, permitted Langer and Flörke (1974a, b) to suppose the existence of two types of molecular water in opaline silica. The first type encompasses individual or non hydrogen-bound molecules in structural interstices; the second one is hydrogen-bound liquid water. In addition, two types of SiOH-groups were recorded. Henceforward, NIRS facilities were used for studying various crystalline forms of silica, both natural and synthetic (Aines et al. 1984, Aines and Rossman 1984, Cordier and Doukhan 1991). The problem of hydrolytic quartz weakening and uncertainties in the OH assignment stimulated further the investigation of water speciation in quartz. The most pressing question is whether hydroxyls are independent OH-groups or belong simultaneously to the molecular water. The data obtained in earlier research cast doubts on the possibility of finding an ultimate answer to this question. First, it was found that the relationship between the intensities $(4500\ cm^{-1})_{SiOH}$ and $(5200\ cm^{-1})_{H_2O}$ combination bands depends strongly on the structural and chemical characteristics of silica phases (Scholze 1959b, Langer and Flörke 1974a). Second, after heat treatment at 500 °C, the "silanol" band at 4500 cm^{-1} and the very intense 894 cm^{-1} and 916 cm^{-1} bands, assigned to disturbance of the SiO_2-lattice by incorporated H-species, disappear (Brunner et al. 1961); simultaneously, the intensity of the water combination mode 5200 cm^{-1} increases. In the process, the quartz sample becomes opaque ("milky"). This implies that H_2O forms from silanol groups. Besides the 4500 cm^{-1} combination SiOH mode, there are other arguments for the tight bonding of hydrogen in silica matrices. Some of these suggest that H is incorporated in the form of molecular water. In H-enriched quartz, Brunner et al. (1961) have recorded very intense 894 cm^{-1} and 916 cm^{-1} bands usually undetectable in pure SiO_2. It was also supposed that these modes might appear as a result of the generation of new modes by the SiO_4- framework when its symmetry becomes decreased through H_2O incorporation. These and related data suggest that the water incorporated into the silica matrix disturbs it.

In this connection, it is of interest to find out how H-defects correlate with trace elements. The fact that water-related defects lower the symmetry of a regular SiO_4 lattice implies that normal chemical bonds arise in defective places. This, in turn, requires foreign ions to compensate charge imbalance. After having examined about 200 samples of alpine quartz, Bambauer (1961) found a correlation between hydrogen and impurities of metals. Then it was shown that a balance $C_{Al} \cong C_{Li + Na + Al}$ exists between minor impurities in quartz (Bambauer et al. 1961, 1962, Rovetta et al. 1989). Kats (1962) showed that the diversity of sharp pleochroic peaks in the 3000–3600 cm^{-1} range are connected with heteroisomorphic $M^+M^{3+} \rightarrow Si^{4+}$ substitution in quartz. He separated $[(Al)_{Si}/H^+]$ and M^+/H (M^+ is alkaline ion) defects. Further investigations disclosed various peculiarities of the concentration and distribution of trace elements in natural and synthetic quartz. A pronounced association between hydroxyl ions and inhomogeneous impurities of metals related to heteroisomorphism M^+M^{3+}(Al, Fe) → Si^{4+} was confirmed by Laudise et al. (1965) and Chakraborty and Lehman (1976). It was also

shown that concentrations of hydrogen and metals vary with growth layers. Aines et al. (1984) and Rovetta et al. (1989) found that hydroxyl exceeds all other impurities. Perny et al. (1992) found that concentrations of Al, Li, and Na vary by more than three orders of magnitude on a scale of tens of micrometres. According to them, such significant variations in impurity contents are caused by the structure of the mineral-forming medium, especially when it undergoes pH fluctuations. There is good reason to identify these impurity inhomogeneities as glassy inclusions, as electron microscopy has imaged numerous Fe-rich nonstructural inclusions of submicron to micron size (Balitskii and Balitskaya 1985). "Gel-like" defects were found in various types of natural and synthetic quartz. The question arises whether the H-defects in quartz are point lattice defects or their aggregates. Brunner et al. (1961), Kekulawala et al. (1978), and Balakirev et al. (1979) studied amethyst, citrine, and some other colour varieties of quartz. They attributed the broad absorption band centered around 3400 cm^{-1}, which does not sharpen into the ice bands at low temperatures, to H-defects in the disordered SiO_2 environment, i.e. to "gel-defects". At the same time, the mode of water and trace element incorporation into these inhomogeneities remained unclear. Peculiarities of the peak at 3400 cm^{-1}, such as large width and isotropic character, point to a disordered aggregate of water-silica defects, imaged by TEM as glassy, nonstructural inclusions. In addition, the abundance of sharp pleochroic peak within the 3000–3600 cm^{-1} range points to crystallographic water defects in crystalline silica. There is much evidence that these defects are closely connected with heteroisomorphic substitution in quartz; Pankrath and Flörke (1989a, b) revealed the fine crystallographic and crystallochemical features of such defects.

An analysis of the views concerning the status of water and trace elements in silica matrices would be incomplete without discussion of the model for hydrogarnet defects. This model was suggested by Nuttal and Weil (1980), who examined α-quartz by EPR and, in addition to the well-studied $[AlO_4/H_4]$ and $[AlO_4]^0$ paramagnetic centres, found two new hole-trapped impurity centers. They were identified as $[H_4O_4]$ and $[H_3O_4]$, respectively. This designation requires the diamagnetic precursor $[H_4O_4]^0$. This presentation of H-defects stimulated further experimental and theoretical work. McLaren et al. (1983) and Cordier and Doughan (1989) accepted this model for water defects as a basis for explaining mechanism of hydrolytic weakening and quartz strengthening after heat treatment at 500 °C. They have written $[H_4O_4]^0$ centers in the form of $[H_4]_{Si}$ (i.e. $4H \rightarrow Si$), and considered them to be embryonic water bubbles ($2H_2O \rightarrow SiO_2$). During heat treatment these bubbles would act as reservoirs for water molecules, which explains the clustering of hydrogarnet defects into numerous submicron bubbles imaged by TEM (McLaren et al. 1989). In the context of these ideas, the atomic mechanism of strengthening, nevertheless, revealed some uncertainties and could not be reduced to the hydrolysis of Si — O — Si bonds suggested by Griggs and Blacic (1965).

Purton et al. (1992), Lin et al. (1994), and McConnell et al. (1995) showed the theoretical agreement of $[OH]_4$ species with proper SiO_2 structures. This is not surprising, as it follows from the existence of such centers in α -quartz recorded by EPR. However, the hypothesis that these defects formed from $4H \rightarrow Si$ substitution is questionable for a number of reasons. Firstly, all 4H involved in these species, according to Nuttal and Weil (1980), are not structurally equivalent. EPR spectra have different hfi (hyperfine-interaction) coefficients (0.068, 0.111, 0.131, 0.230 mT). This means that every "H" comes from various H-defects; therefore, the $4H \rightarrow Si$ substitution scheme does not work. Secondly, the authors themselves defined $[H_4O_4]$ species as a preliminary model, which required further investigation. A genetic relationship was supposed between $[AlO_4/H]^+$ and $[OH]_4$ species, which implies that trace elements were involved in hydrogarnet defects. The model for hydrogarnet defects thus brings up many new questions.

Summarizing all these data, we can conclude that water-related defects in quartz and other silica minerals reveal themselves as H_2O, OH, and H more or less bound with the SiO_2-matrix. They may have crystallographic and/or disordered lattice environments and commonly are associated with trace elements incorporated in the quartz framework. Finally, the H-defects may manifest themselves as point defects or their disordered aggregates. All these features have been detected by experimental methods and in some cases have been confirmed theoretically. It can be said that the character of H-defects is elusive where the boundary between H and H_2O is not well defined (Kronenberg 1994).

Experimental

Approach

A review of data published in the literature shows that water-trace element defects are the most characteristic lattice imperfections in quartz. There is also evidence of grow-in nature of these defect species. A wide range of these defect types, especially those that concern the water constituents, depends strongly on quartz genesis and its post-crystallization history. This means that the questions concerning water and impurity speciation in the SiO_4 lattice can be answered only by studying various genetic types of natural quartz. Another argument for this approach is that the knowledge of the actual structure of quartz, the most widespread rock-forming mineral, is of great importance for solving genetic problems. This is especially true for the vein quartz with ore mineralization. For this reason, we have attempted to resolve the actual structure of specific types of natural quartz, although their defect patterns are often very complicated. On the other hand, this complexity may be of practical importance since the genetically most informative defects would be better understood when analyzed together with other microstructural features. This follows from the growth nature of defects and their mutual interaction during the post-crystallization history of minerals and rocks.

Sampling

Quartz exhibits a great variety of forms in nature. This is due to various modes of water and trace element incorporation into the silica matrix. Properties such as colour, transparency, degree of crystallinity, and many others depend on quartz microstructure. The most thorough classification of quartz is based on its origin and ore specialization. The present study summarizes the data obtained for quartz of hydrothermal, magmatic, and pegmatitic origin (Stenina et al. 1984), vein quartz with Cu-Mo mineralization (Stenina et al. 1988), and various types of gold-ore quartz (Stenina et al.1993, Stenina et al. 2000). Gangue quartz was also studied.

Valuable information can be obtained from the vein quartz related to ore mineralization. This quartz displays several generations (up to 5–7) differing in transparency, colour, textural features, specific gravity, and other physicochemical properties (Yurgenson 2003, Müller et al. 2003). The number of generations correlates positively with the vein productivity (Stenina et al. 2000). The most distinct differences in the chemical and physical structure are observed between grey transparent quartz (denoted below as Q1) and milky-white opaque quartz (Q2) (Fig. 1).

Methods

A number of methods were used toward characterizing the H-related defects in quartz. Each method was chosen for its specific applicability to studying the nature of a complex defect. Both local (TEM, X-ray microprobe) and integral (IRS, TG, X-ray powder diffraction, EPR) methods were employed.

Light microscopy shows the close structural and textural relations between quartz modifications and ore phases within vein quartz. This micrometre-scale investigation is necessary for choosing a sample for subsequent examination by TEM methods. **TEM** (high voltage JEM-1000 and high resolution JEM-4000EX electron microscopes were used) was our leading method, since it is the only direct tool for the imaging and crystallographic identification of lattice defects. TEM enables the imaging of general pattern of structural imperfections in the quartz matrix, the recording of interrelations between various defects, and the crystallographic characterization of the defects. These data permit one to classify the defect as a known type (dislocation, twin boundary, inclusion, etc.), or to obtain the key information needed for the identification of a previously unknown type. Quartz samples have been prepared for TEM analysis from mineral thin sections by ion thinning. ***Infrared spectroscopy*** (IRS; SPECORD-75) was used to gain information on the state of water in the silica matrix (H_2O, OH, crystallographic H-defect or H-defect in disordered lattice environment). ***Thermogravimetry*** (TG; thermogravimeter G 50 Mettler GA 300) gives information on the total amount of water in quartz and the water-SiO_2 bonding energy. The structural state of quartz was characterized by means of X-ray powder diffraction (diffractometer URD – 63). Concentrations of trace elements were determined by atomic-absorption spectroscopy (**AAS**; spectrophotometer SP-9). In our earlier work (Stenina et al. 1984; Stenina 1987; Stenina et al. 1988) we also used ***electron paramagnetic resonance*** (EPR) and ***X-ray microprobe*** analysis. EPR yields information on point defects: substitution and/or interstitial foreign atoms (AlO_4^{4-}, Ge^{3+}(C), Ti^{3+}/Na paramagnetic centers) and vacancies (E`-centers). X-ray microprobe allows the imaging of trace element inhomogeneities in the silica matrix a few microns in size.

Experiments were made in order to study the behaviour of water and trace elements in quartz lattice at elevated temperatures. According to previous data (Bazarov and Stenina 1978), the critical temperature for altering the water-impurity defects in quartz is about 500 ° C. Therefore, the specific samples were held at 500 °C (in some cases at 700 °C) for tens (10 to 100) of hours. Then they were cooled either by annealing or quenching.

Results

Light microscopy

Investigation with light microscopy showed that magmatic and hydrothermal varieties of quartz have a relatively homogeneous inner structure. The same is true for hydrothermal vein quartz with minor mineralization. On the contrary, the vein quartz associated with economic mineralization displays significant variability of textural features (Fig. 1). Concerning its structural and chemical state, two main gradations may be distinguished. The first implies a sharp difference between dark-gray transparent (Q1) and milky-white (Q2) quartz. In poorly mineralized veins, Q2 generally constitutes a vein body. Economic veins are composed of different quartz varieties. A significant proportion of these bodies is represented by Q1 varieties, whereas Q2 is immediately associated with ore phases (sulphides, native gold). The second gradation relates to grey transparent quartz. This quartz is subjected to strong structural and textural transformations near the ore phases. These interrelations suggest that ore phases were isolated by structural and chemical transformations within the complex silica matrix.

Transmission electron microscopy

TEM is a useful tool for identifying lattice defects, and is therefore necessary for understanding the mechanisms by which these transformations occur.

TEM examination has revealed characteristic defects common for most modifications of natural and synthetic quartz. They have a complicated diffraction contrast, a major feature of which is two sets of lobes symmetrically placed about the so-called line of no contrast (Fig. 2a). These defects have attracted considerable interest over the past two decades because there is evidence of their direct relationship with water-related defects in quartz. In interpreting these

features, many investigators use the findings of Ashby and Brown (1963a, b), who showed that a lobe diffraction contrast is due to the strain field around plate-like precipitates in metallic alloys. In quartz the nature of lobe-contrast defects is not so evident. There exists a wide diversity of viewpoints on their character. Morrison – Smith et al. (1976) attributed the lobe contrast to microscopic solid inclusions, probably acmite ($NaFeSi_2O_6$). McConnell et al. (1995) interpreted them as planar defects. McLaren et al. (1983) observed dislocation loops generated by these defects, which, in their opinion, are tiny water-containing bubbles. Cordier and Doukhan (1991), however, considered the lobe-contrast defects as "hydrostatic pressure centers which should be called clusters or aggregates rather than fluid inclusions".

Our observations show that the fine peculiarities of these defects strongly depend on the mode of origin of the quartz (Fig. 2). Hydrothermal quartz (Fig. 2a) has the highest density of these features (about 10^{11} cm^{-2}); the smallest of them (0.01–0.02 μm) looks like a double arc with the line of no contrast (LC) having the same direction as the rest of the defects, which is perpendicular to the basic active reflection (Fig. 2a, inset). According to Hirsch et al. (1968) such contrast features allow the defects to be interpreted as thin platy segregations located in the same plane. In magmatic quartz, the lobe-contrast defects are closely associated with the dislocation network (Fig. 2b). The wide diffraction contrast of dislocations suggests their decoration by impurities. This means that the atoms of trace elements are precipitated at the broken bonds in the dislocation cores. Quartz from pegmatites shows a more complex pattern of microstructure (Fig. 2c). Lobe-contrast features disappear in the matrix enclosing gas-liquid bubbles. Structural imperfections here are arranged concentrically around the pore (marked 2 in Fig 2c). In an electron microscopic image, they are visible due to the strain contrast of the host matrix (Fig. 2c – 1). Larger defects of 0.5–0.7 μm in size (Fig. 2c – 3) are visible due to their own diffraction contrast. According to Hirsch et al. (1968) and Baker (1970), coherent precipitates of a new phase in exsolved metal alloys have such a contrast. The close similarity between the diffraction contrast of quartz defects to those in alloys suggests that the former can also be interpreted as coherent precipitates. Vein quartz related to ore mineralization displays various defect patterns. The lobe-contrast defects are typical of gray transparent quartz. Here, the defects have sizes from one to several tenths of a micrometer (Fig. 2d). The diffraction contrast of some of these defects strongly resembles those of tiny "voids" (Heydenreich 1969) or lenticular glassy microinclusions.

In addition to the lobe-contrast defects, almost all quartz samples have specific features a few microns in size (Figs 2c – 4, e). These defects with absorption contrast in the TEM image and an irregular interface with the host matrix seem to be glassy (gel-like) inclusions in the quartz.

Rare quartz samples having no lobe-contrast defects were found in non- or poorly-mineralized veins, and among quartz generations within highly productive ore

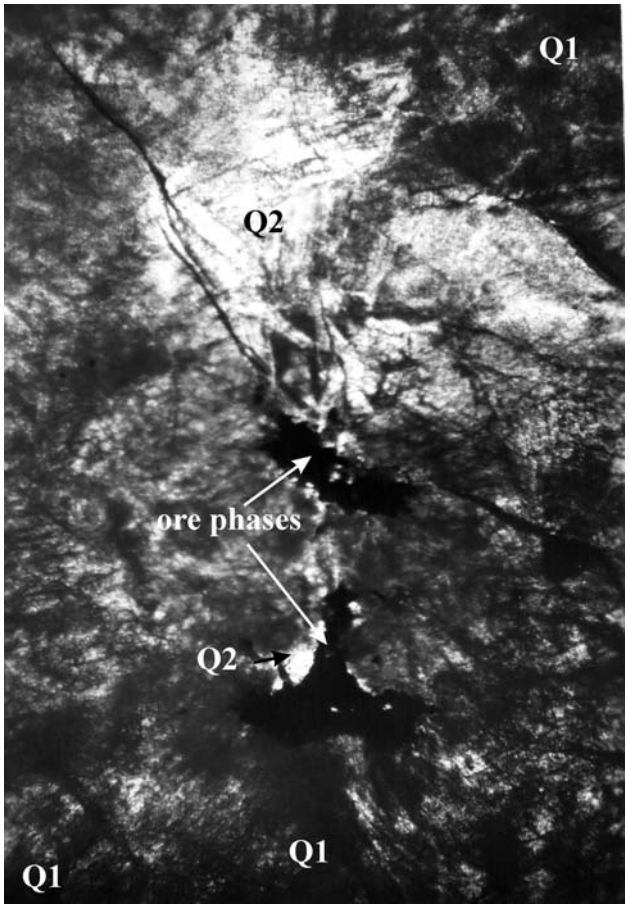

Figure 1. Optical micrograph of vein quartz related to gold-sulphide mineralization; Q1, Q2 denote quartz generations, ore phases are metallic sulphides (Fe, Cu, etc.).

veins. In the latter case, it is specifically Q2 (Fig. 1) that is immediately associated with ore phases. The characteristic feature of its microstructure is presence of water-containing bubbles (Fig. 2f), which implies free water incorporated in the matrix. This condition serves as an indirect indication that the water in quartz with lobe-contrast features occurs in a chemically bonded form.

The lobe-contrast defects significantly contribute to the unusual phenomenon of quartz amorphization under electron irradiation during TEM observation. McLaren and Phakey (1965, 1966) first reported this phenomenon in the case of amethyst and citrine quartz. Since then, no information about quartz amorphization has appeared in the literature. However, our observations unambiguously show that disorder in the quartz crystal lattice under electron irradiation is directly related to water and trace element speciation in the silica framework. The following considerations support this statement.

Firstly, amorphization of the crystal lattice begins in the lobe-contrast defects (Figs 3a, b). In other words, these features are centers in which a crystal lattice looses its order (compare Fig. 3a with Fig. 2a). Changes in the electron-microscopic image proceed in the following steps: 1) blurring of the distinct lobe-like contrast, 2) appearance of tiny water bubbles (Fig. 3b) and numerous black dot contraction features (< 100 Å in size); the latter is especially typical of

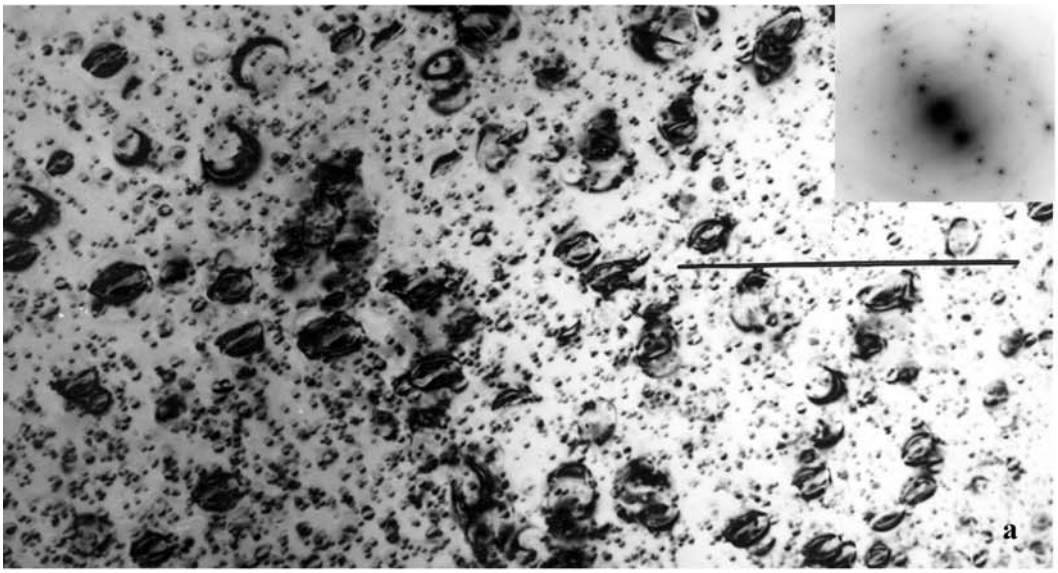
a

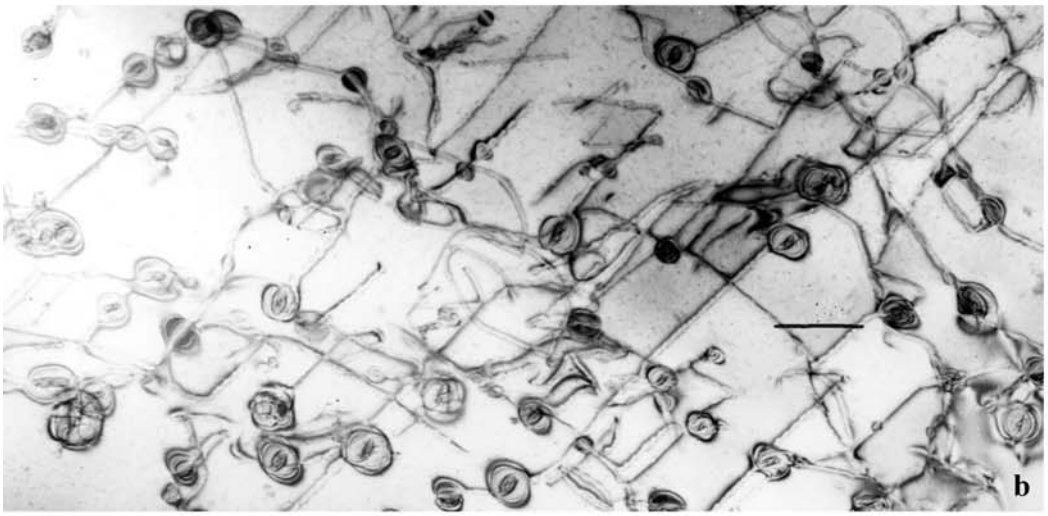
b


3
4
4
1
2
c

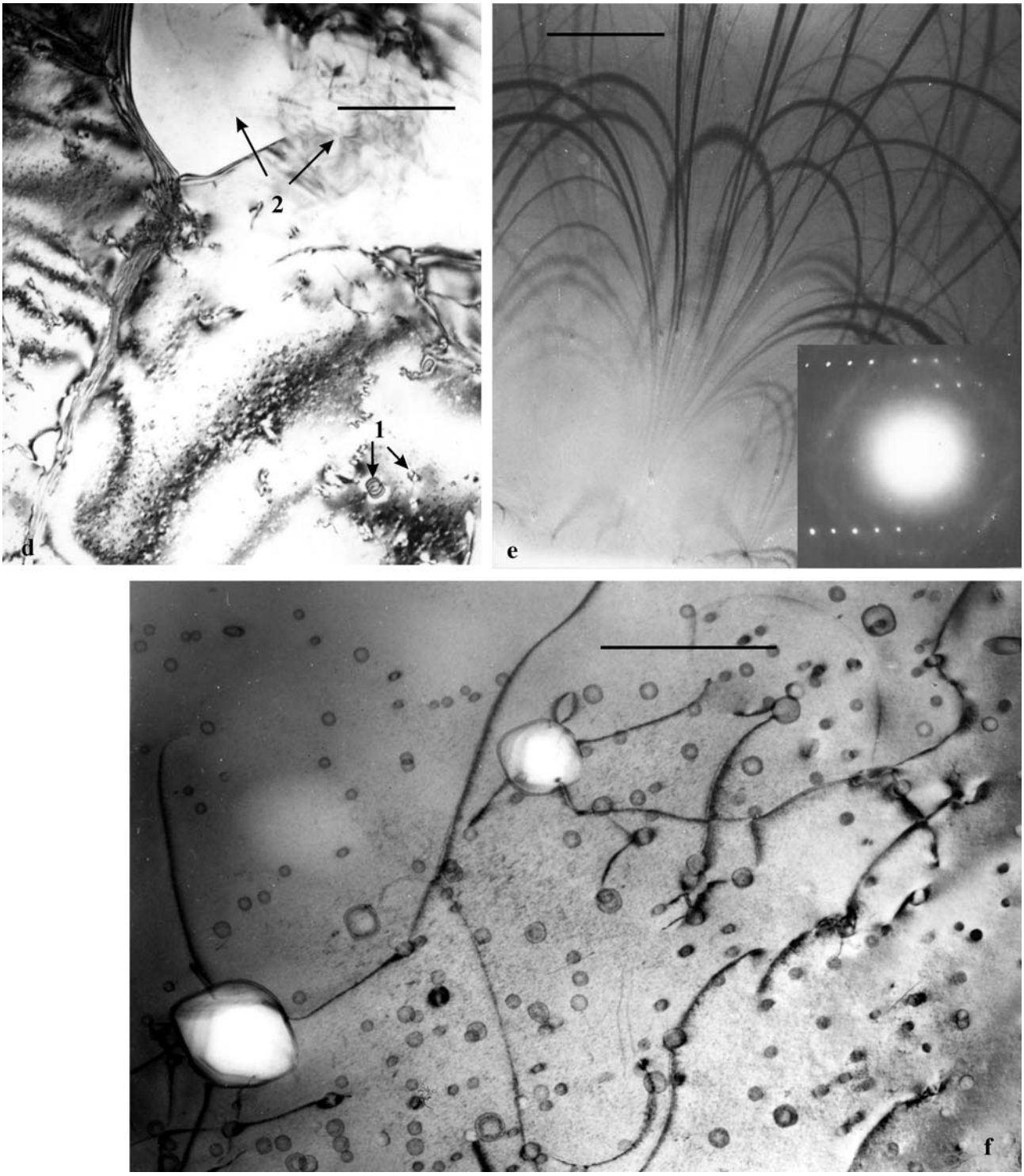

←↑
Figure 2. TEM images of microstructural features in quartz of different origins (scale bar is 1 μm): a – hydrothermal: lobe-contrast defects (microdiffraction pattern is in the inset); b – magmatic: lobe-contrast defects are associated with dislocations; c – quartz from pegmatites: (1) tiny inclusions with strain contrast of host matrix, (2) location of gas-liquid bubble, cut during ion-thinning, (3) coherent precipitates, (4) gel-defects; d – generation of vein quartz associated with ore mineralization: lobe-contrast-defects (1) and blocks of recrystallization (2); e – gel-defects of micrometre size in hydrothermal quartz (microdiffraction pattern is in the inset); f – water-containing bubbles in poorly mineralized vein quartz.

ore vein quartz, 3) disappearance of all contrast features and amorphization of the bulk specimen during several minutes of observation.

Secondly, the amorphization of a crystal matrix is accompanied by the liberation of water therefrom. This is supported by the appearance of tiny water-containing pores during the first few minutes of electron irradiation (Fig. 3b) and, most apparently, by a simultaneous increase in the volume of gas-water bubbles and amorphization of the host matrix (Figs 3c, d). This suggests that a lack of quartz

crystallinity is caused by the liberation of volatiles (most probably H_2O) from the SiO_4 framework. The appearance of abundant black dot contrast defects (Figs 9b, c), which are most likely clusters of trace elements, evince that they are released from the quartz matrix during its amorphization simultaneously with water.

Third, the time required for the total amorphization of the specimen depends on the origins of the quartz. Hydrothermal quartz comes to an amorphous state the most rapidly (1–3 minutes); quartz from pegmatites becomes totally amorphous in 6 minutes; different generations of ore vein quartz take various times to transform into an amorphous state. Magmatic quartz does not lose its crystalline structure. These observations allowed us to exclude damage effects during electron beam-crystal interaction from the possible reasons of quartz amorphization.

Thus, amorphization is linked to water and impurity speciation in quartz. Heating experiments also contribute understanding this phenomenon. Hydrothermal quartz quenched after heat treatment has minor concentrations of structural imperfections (Fig. 4a), though they were abundant in the original sample (Fig. 2a). This quartz does not become amorphous under electron beam. In annealed quartz, lobe-contrast features reappear (Fig. 4b). They are closely related to as-formed dislocations. Besides, tiny water bubbles are threaded upon dislocations. On the basis of these data, we can conclude the following: the lobe-contrast defects have an elevated content of chemically bound water and trace elements; the formation of dislocations is caused by their liberation from the silica framework; as-formed dislocations act as pathways for water and impurity migration (Heggie 1992) and secondary precipitation.

In summarizing the TEM data, we can argue that water and trace elements are combined within the lobe-contrast and larger gel-like defects (Fig. 2). Judging from the contrast features (diffraction and absorption correspondingly), these impurity inhomogeneities in quartz are most likely lenticular (submicrometre) or irregularly-formed (several micrometres) inclusions of gel-like matter. However, TEM alone cannot inform us as to the form in which water and trace elements are incorporated into quartz, or how they are bound with one another and with the SiO_4 framework. Information for answering these questions must be obtained by other methods.

IRS, TG, AAS, X-ray methods, EPR

Three main questions arise from our discussion of the TEM data:

1) Concerning water, it is necessary to find out whether H_2O is incorporated only into the impurity gel-like defects and/or is uniformly distributed over the silica matrix. It is further of interest to discern the water speciation (H, OH, H_2O), and the character of its bonding with trace elements and the [SiO_4] units in the quartz framework.

2) Concerning the trace elements (hereafter denoted as M), it is of principal importance to identify them and to elucidate their crystallographic positions in the quartz structure (substitution or/and interstitial atoms).

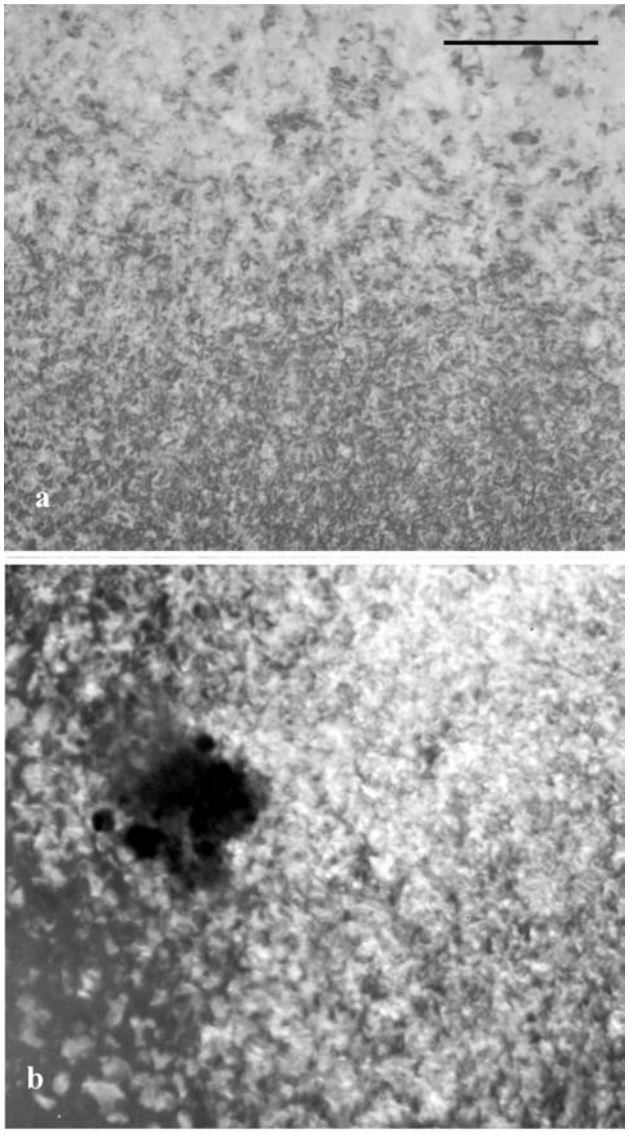

Figure 3. Amorphization of quartz crystal lattice under electron beam (scale bar is 1 μm):
a, b – coincidence of centers of amorphization with the lobe-contrast defects: hydrothermal quartz exposed to electron irradiation for 1.5 and 2.5 minutes, respectively; (b is dark-field image; water bubbles are black).

3) The third question is the significance of the amorphization of crystalline quartz under electron irradiation. The available publications on quartz do not address this phenomenon. However, the above analysis of its characteristic features (Fig. 3) seem to be encouraging toward solving this problem.

IRS and TG have shown a fundamental distinction in the state of water between quartz with lobe-contrast and gel-like defects, and quartz with water-containing bubbles. Q1 and Q2 are the most prominent representatives of these two groups. Both of them (Fig. 5, solid lines) have a broad peak centered at about 3400 cm^{-1} in the IR-spectra. Brunner et al. (1961) and Kekulawala et al. (1978) attributed this peak to molecular H_2O being incorporated into the disordered silica matrix. The most important point is that at a low temperature (77 °K) almost all of the intensity of the 3400 cm^{-1} peak for Q2 shifts to the ice band at 3200 cm^{-1},

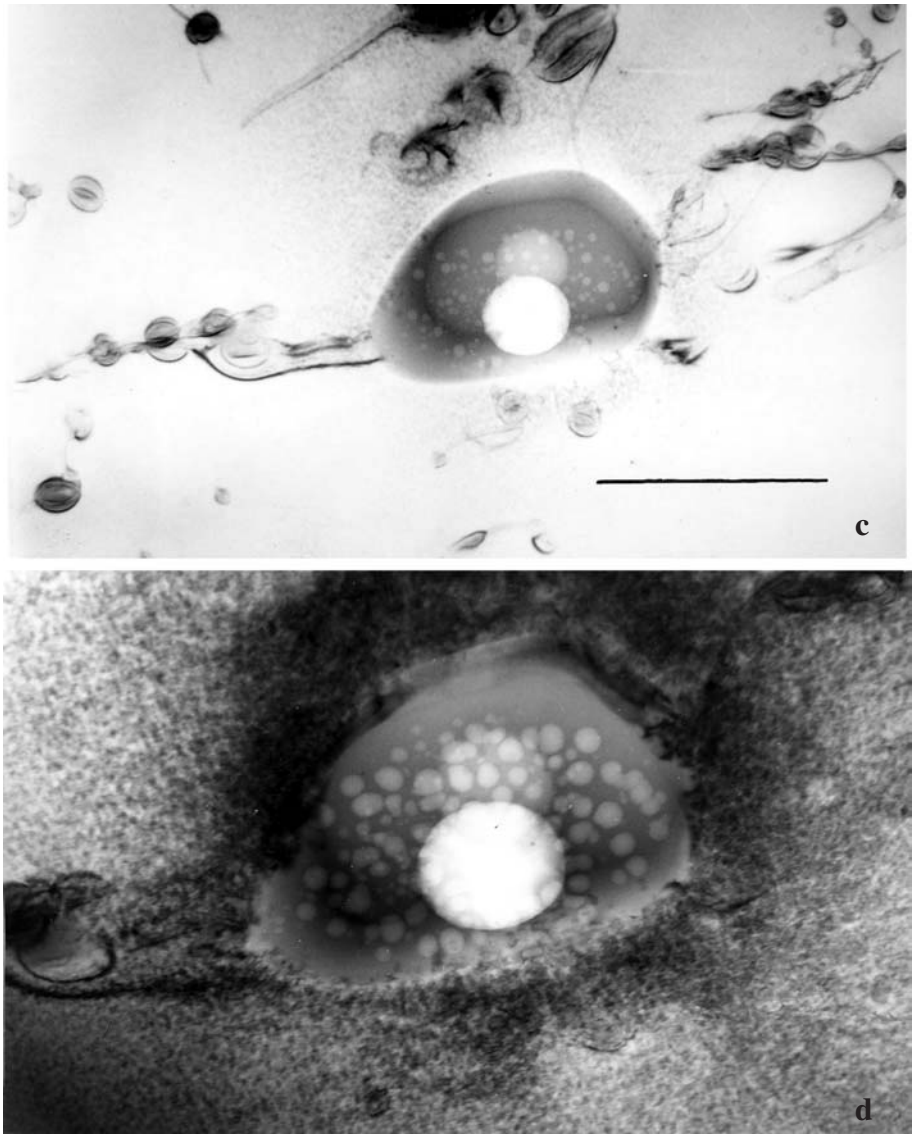

Figure 3, continued:
c, d – alteration of gas-liquid inclusion and host matrix upon electron irradiation (hydrothermal quartz): (a) – faceted pore with a gas-liquid content at the onset of observation, (b) – simultaneous increase in inclusion volume and amorphization of host matrix after 6 minutes of observation under an electron beam.

whereas in Q1 the intensity of this peak is redistributed between the 3400 cm^{-1} and 3200 cm^{-1} bands (Fig. 5, dashed lines). This means that Q1 contains both chemically bound and free water, whereas Q2 contains mainly free water in bubbles.

TG has supported this conclusion. On heating, Q1 and Q2 show a fundamentally different character of water loss (Fig. 6). One narrow intense peak at 650 ° C (Fig. 6a) indicates that in Q1 molecular water occupies mostly the structural positions of the silicon-oxygen framework and forms chemical bonds with it. Q2 displays two diffusive peaks of low intensity at about 250 °C and 450 °C (Fig. 6b). The molecular water responsible for these peaks seems to occur in a free and adsorbed form in channels of quartz structure, tiny pores, microfractures, and other mechanically weakened zones of quartz bulk. The total amount of water in Q1 is 2.5 times greater than in Q2. These data allow us to define the water of transparent quartz varieties as structurally bound and highly energetic, and the water of milky-white quartz as free and/or weakly bound. The universal character of this designation is confirmed by the data previously obtained for quartz varieties from the ore veins with Cu-Mo mineralization (Stenina et al. 1988), which showed the same behaviour of broad 3400 cm^{-1} band.

AAS data also show that Q1 and Q2 distinctly differ in their concentrations of trace elements (Table 1).

Thus, Q1 and Q2 differ markedly in their contents of gold and silver. Among multivalent cations of Fe and Al, iron correlates with gold better than Al does.

X-ray microanalysis was used with two aims: (1) to record trace elements entering the gel-like inhomogeneities, and (2) to evaluate the contribution of heteroisomorphic $M^{+}M^{3} \rightarrow Si^{4+}$ substitution into the formation of these defects. Quartz from pegmatites and hydrothermal quartz are the most appropriate for this purpose because of the complex configuration and sizes of their impurity defects. Back scatter X-ray images of the optically visible gas-liquid inclusions in the thin sections of pegmatite quartz showed aluminium and sodium concentrated around the inclusions, though there is no complete correspondence in concentration and distribution between these elements (Figs 7a, b). Such a pattern suggests that aluminium atoms occupy fixed positions in the quartz lattice (most likely $Al^{3+} \rightarrow Si^{4+}$ within the oxygen tetrahedron); sodium, as an ion-compensator, enters the interstitial position by the $[AlO_4]$ tetrahedron. It is reasonable to suppose that along with sodium, other uni- and bivalent elements (Li, K, Fe^{2+}, etc.) and H^{+} can be incorporated into defects in the silica lattice for compensating charge deficiencies by forming a $[M^{3+}O_4]$ tetrahedron. From comparing the TEM image of the pegmatite quartz (Fig. 2c) with its X-ray image (Fig. 7a, b), it may be concluded that Na, $M^{+}(H^{+})$, $Al^{3+} \rightarrow Si^{4+}$substitution takes place in small defects enclosing the gas-liquid

Table 1. Concentrations of trace elements in vein quartz (ppm)

Quartz	Au	Ag	Fe	Al	Na
Q1	5.23	4.29	1660	1820	146
Q2	0.04	0.18	900	1620	52

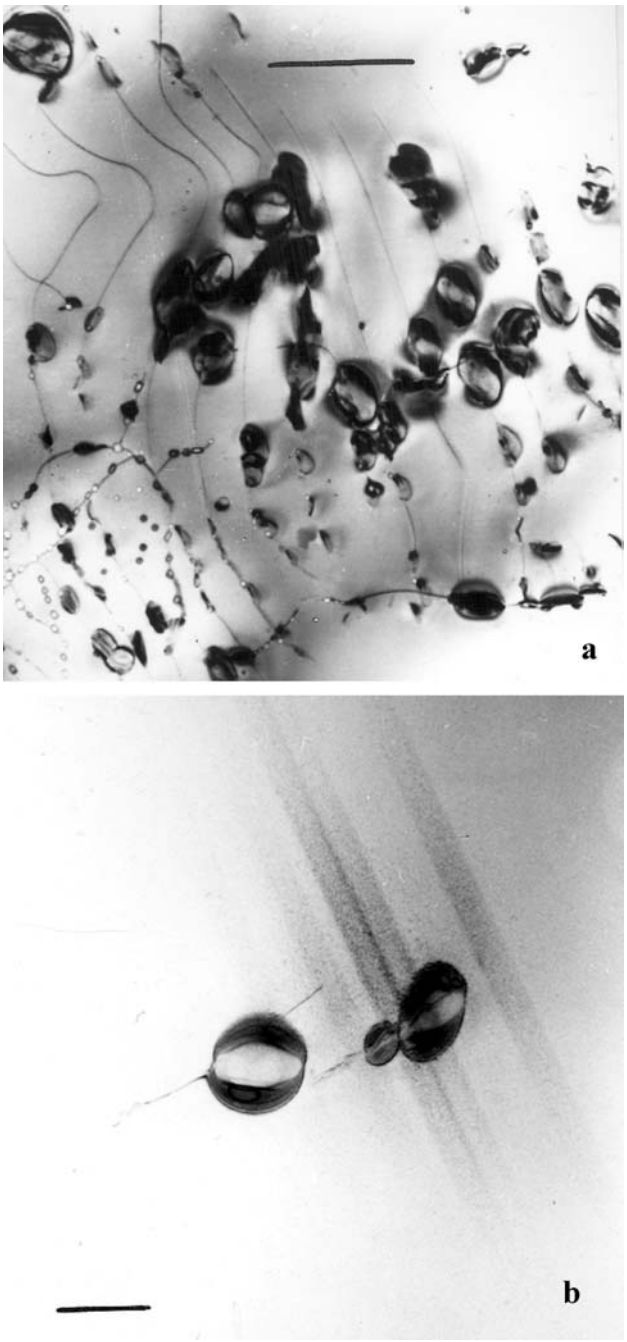

Figure 4. Microstructure of hydrothermal quartz heated to 500 °C during 100 hours, and cooled by quenching (a) and annealing (b) (scale bar is 1 μm).

inclusions of micron size. The location of one of them is marked by 2 (its corresponding gas-liquid bubble was cut during ion thinning of the sample). In addition to Na Al → Si, X-ray microanalysis has demonstrated that Mo → Si and Au Fe → Si replacements in quartz are related to Cu-Mo (Stenina et al. 1988) and Au-sulphide (Stenina et al. 1993) mineralization, respectively. Figures 7c and d show that gel-defects are enriched with trace elements, and the M^{3+} position is occupied by Al and Fe equally.

X-ray powder diffraction also provides information on the character of trace element incorporation into the silica framework. Q1 and Q2, contrasting in the concentrations and state of water and trace elements, have easily distinguishable diffraction patterns. In Q1 the diffraction peaks (212), (203) and (201) are poorly resolved (Fig. 8a), whereas in Q2 they are sharp (Fig. 8b). Broadening X-ray diffraction lines may occur for two reasons: 1) the availability in the sample of small (less than 1000 Å in size) blocks of coherent scattering, and 2) statistical deviations of interplane distances from the exact d value for α-quartz. In the present case, the superposition of peaks in the X-ray pattern of Q1 is caused by the second reason. TEM data have shown (Stenina et al. 2000) that microblock structure is typical mostly of Q2, its substructural blocks being considerably larger than the critical parameters (~ 1000 Å) for blocks of coherent scattering. Hence, the poor resolution of diffraction lines in Q1 results from microdistortions of crystal lattice, i.e. deviations of the interplane distances of the gray transparent Q1 from the d values of chemically pure SiO_2 (quartz). After the annealing of Q1 at 700 ° C (10 hours), which is higher than the release temperature of chemically bound water (650 °C, Fig. 6a), the appearance of its X-ray pattern resembles that of Q2. X-ray data suggest that water and trace elements are crystallographically incorporated in the transparent quartz varieties exhibiting lobe-contrast defects. The observation of quartz behaviour under the electron beam in an electron microscope (Fig. 9) confirms this conclusion. During the first moments, the quartz lattice as visible from microdiffraction (Fig. 9a, inset) has a strained appearance. After 5 minutes of electron irradiation, abundant black-dot contrast features arise in the TEM image of the sample, and the microdiffraction pattern arranges itself symmetrically (Fig. 9b). Analyzed together with X-ray powder diffraction data, these observations evince the relaxation of lattice strain. After 7 minutes of electron irradiation, the quartz matrix becomes amorphous (Fig. 9c). In milky-white non-transparent quartz, water is not bound with trace elements and mainly occurs in a free form within bubbles (like those of Fig. 2f).

The next question to be answered is related to degree of agglomeration of the combined water-trace element defects in quartz. We wish to know whether they occur only as disordered or poorly-ordered aggregates (gel-like defects), or are they single species incorporated crystallographically. TEM gives unambiguous information on the clusters of such impurity defects, starting from sizes of several tens of Å. Concerning point defects, TEM can record any indirect manifestations but it cannot resolve them. In this case the use of EPR is appropriate. EPR records the paramagnetic centers in crystal lattices, which result from the substitution of foreign atoms into the Si position ($M^{3+} \rightarrow Si^{4+}$), from the incorporation of M^{+} into the interstitial positions, and from vacancies in the crystal lattice. According to the EPR data, hydrothermal, magmatic and pegmatitic quartz have high concentrations of paramagnetic defects (Stenina et al. 1984). They were identified as $[AlO_4]^{4-}$, Ge^{3+}(C), and Ti $^{3+}$/Na centers originating from $M^{+}M^{3+} \rightarrow Si^{4+}$ substitution. In addition to these, the abundance of so-called E`-centers have been found. Weil (1984) showed that E` paramagnetic defect results from a

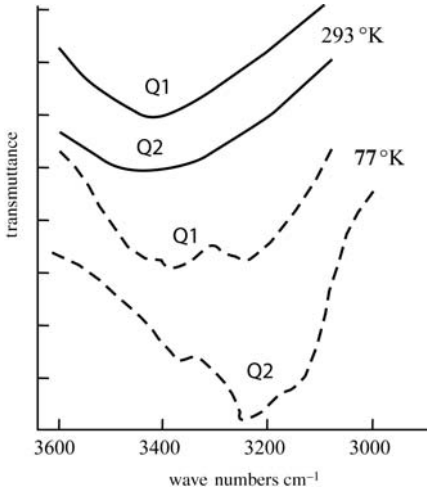

Figure 5. Fragments of IR-spectra of Q1 and Q2 with a wide diffusive band about 3400 cm^{-1} (solid lines refer to registration at 293 °K, dashed lines at 77 °K).

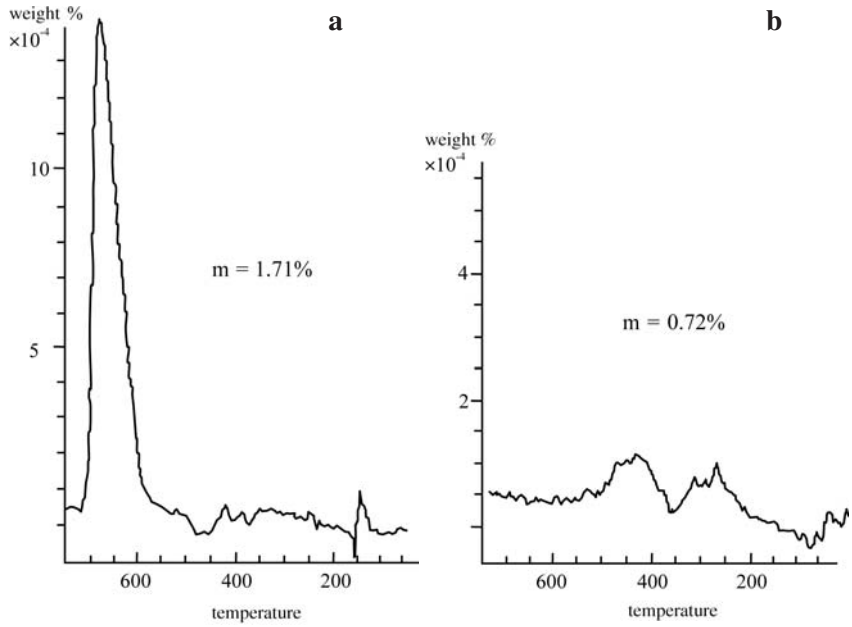

Figure 6. Curves of water loss of Q1 (a) and Q2 (b) on heating.

vacancy left by an O^- ion missing from a normal bridging oxygen location, with consequent relaxation of the position of the silicon neighbours. This point is emphasized, as it is important in the further construction of the model for water and trace element incorporation in the quartz framework. The EPR data agree well with the TEM observations. The homogenization of water-trace element segregations after heat treatment is expressed in a four-fold increase in the concentration of AlO_4 centers. All of these data indicate that quartz traps water-trace element complexes not only as disordered segregations but also as single units, which were built into the SiO_4 framework crystallographically. Peculiarities of the amorphization process support this conclusion. Electron microscopic images in Fig. 3 show that after having started at the impurity-saturated sites, amorphization extends to cover the bulk of the sample. Quartz with higher concentrations of water undergoes total amorphization of its structure within two to three minutes.

Summarizing the data obtained by various methods, we can state that they are sufficient for constructing a model for the combined water-trace element defects in quartz.

Model for water-trace element defect in quartz

The data obtained by TEM and other methods suggest the following conclusions concerning water and trace element incorporation into quartz matrices.

1. Water and trace elements are combined together within complex defects.
2. Trace elements enter defects by heteroisomorphic substitution $M^+M^{3+} \rightarrow Si^{4+}$ ($M^{3+}M^{5+} \rightarrow 2Si$).
3. Water and trace elements are incorporated into the quartz lattice crystallographically as single species, and noncrystallographically as gel-like (glassy) inclusions of submicron or micron size.
4. Chemical bonds are broken and impurity inhomogeneities are destroyed at temperatures above 500 °C.
5. There is a relation between the disintegration of defects and the formation of dislocations in quartz.
6. Single water-trace element defects and gel-like segregations are grown-in.
7. Water and trace elements are most likely chemically bound with SiO_4 units in crystallographic and gel-like defects.

All these data, analyzed together, suggest that there is a combined $[SiO_4] - H_2O - M^+[M^{3+}O_4]$ defect. The nature of its grown-in nature implies that these species are structured units of mineral-forming media, trapped into the quartz bulk during crystallization. Silica-water-impurity complexes may be built into the quartz framework crystallographically, yielding point defects that are identifiable by EPR. Disordered clusters of these species are incorporated in the quartz bulk as gel-like defects. The proportion of such clusters in quartz is inversely related to the temperature of crystallization. A general pattern of distribution of these species in quartz matrices is shown in Fig. 10a. During the post-crystallization history of a mineral these species disintegrate to form complex defect configurations, as can be seen in quartz from pegmatites (Fig. 10b; compare with Fig. 2c). Here, along with disordered clusters of water-impurity (gel-like) defects (marked by Fig. 4), there are inclusions of ordered species (Figs 1, 3). Small coherent inclusions are marked as"1" host gas-liquid inclusions. Such defect configurations suggests that they result from the disintegration of $[SiO_4] - H_2O - M^+[M^{3+}O_4]$ species within the initially disordered

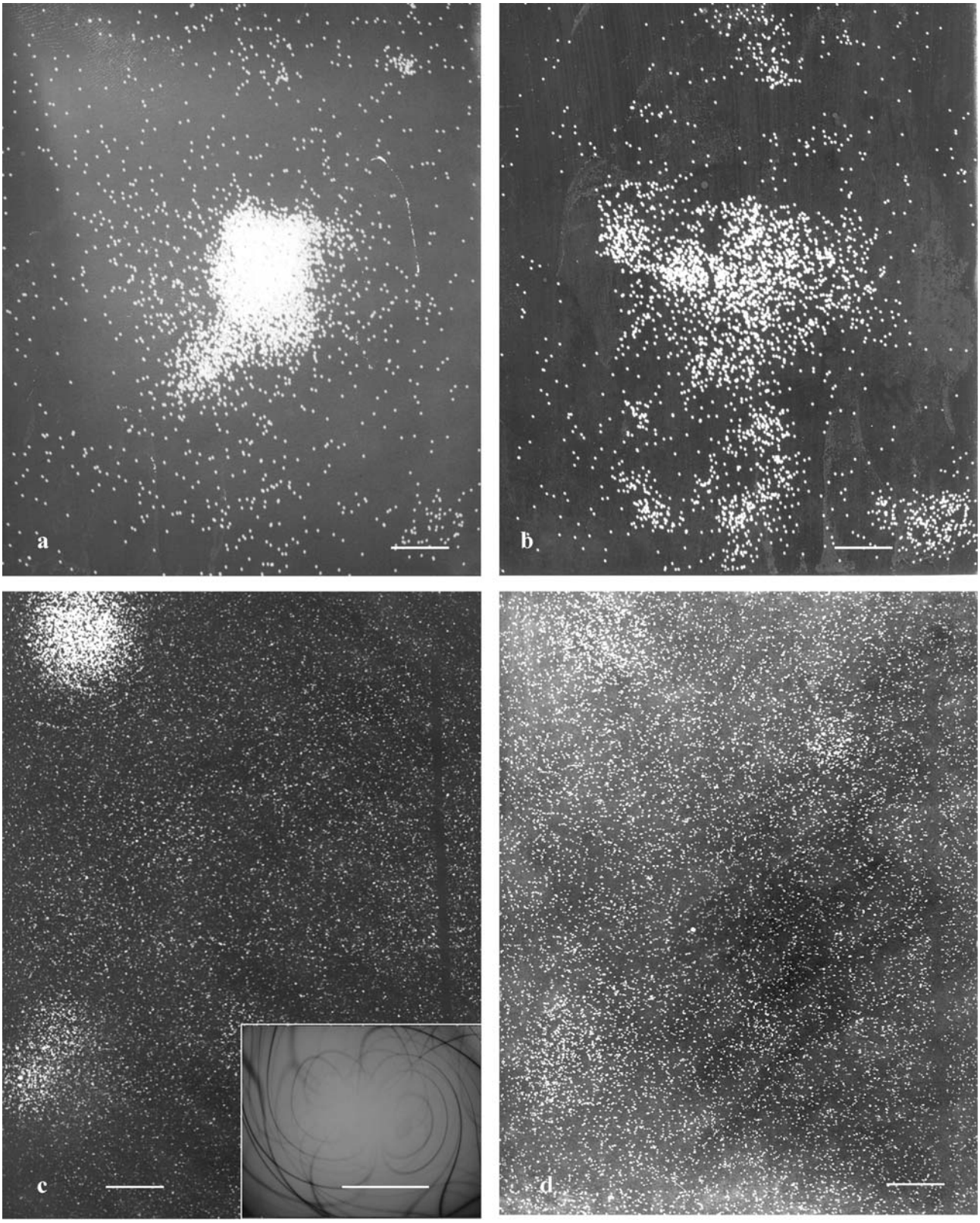

Figure 7. Back-scatter X-ray images of thin sections:
a, b – quartz from pegmatites; micro-areas around gas-liquid inclusion: AlK_α (a) and NaK_α (b) (scale bar is 10 μm).
c, d – gel-like defects of micron size in hydrothermal quartz: AlK_α (c, TEM image is in the inset), FeK_α (d), scale bar is 1 μm.

clusters. The water liberated from gel-like defects is concentrated in tiny pores, most likely as a result of the clustering of vacancies in the quartz lattice. In the process, the pores grow into water-containing bubbles several micrometres in size. Simultaneously, the remaining $[SiO_4]$ and $[M^{3+}O_4]$ tetrahedra come into order. Finally, this results in the formation of

coherent inclusions. Such defects represent the phase having quartz structure but the lattice parameters, differing from those for pure α-quartz because of $M^+M^{3+} \rightarrow Si$ (also $M^{3+}M^{5+} \rightarrow 2Si$) substitution. Berlinite ($AlPO_4$) is an example of such substitution. Diffraction contrast in the silica matrices that host such micro-inclusions (Fig. 2c – 1, 3) tends to confirm this mechanism.

The major point related to the combined $[SiO_4] – H_2O – M^+[M^{3+}O_4]$ defect concerns water speciation. Specifically, does water enter in the molecular form or is it present as hydroxyl ions? Abundant IRS data in the literature evidences both kinds of speciation. At the same time, the crystallochemical view of these complex defects depends on solving this problem. Quartz amorphization under electron irradiation during TEM examination of the sample gives key information for understanding water incorporation in the silica framework. First, one needs to understand the mechanism of amorphization itself. An electron beam being transmitted through a thin crystalline foil is divided into elastically scattered and inelastically scattered electrons. Elastically scattered electrons are reflected from atomic planes as they are transmitted through the foil, and form a diffraction pattern. Inelastically scattered electrons loose their energy and are absorbed into the crystalline sample. These latter electrons seem to cause amorphization. Taking into account that amorphization is accompanied by water escape from the crystalline matrix, one can assume that the incorporation of H_2O molecules into the SiO_4 framework produces electron-unsaturated chemical bonds. It should be kept in mind that water is a charged tetrahedron (Bernal and Fowler, 1933). According to the sp^3 – hybridization of electron bonds (Fig. 11a), the H_2O molecule has a tetrahedrally charged structure (Fig. 11b). Two corners of the tetrahedron are occupied by the positive charges of protons (H^+), while the electron density from the oxygen of the water molecule is located in the other two corners. The tetrahedral angle of water molecules (105°3') is close to that of the $[SiO_4]$ tetrahedron (104–105°). This similarity suggests their tetrahedra would fit well together in the framework of quartz structure. For achieving charge balance in such a defect, the oxygen of a water molecule must serve as a bridge oxygen between two $[SiO_4]$ tetrahedra and to bind $2H^+$ through hydrogen bonds with two deficient $[M^{3+}O_4]$ tetrahedra. A crystallochemical scheme of such a defect is given in Fig.12a (Fig. 13a illustrates amorphization). Correspondingly, the formula of the defect must be written as $[2SiO_3 \square - OH_2 – M^{n+}M^{m+}O`_4]$ (where $\square$ is an oxygen vacancy, $n = 1,2$; $m \geq 3$). In the left part, the oxygen of a water molecule entering the bridge position in Si — O — Si forms two donor-acceptor bonds with the neighbouring silicon atoms. These bonds are electron-unsaturated and weak. In the right part, two H^+ form hydrogen bonds with the oxygens belonging to two $[M^{m+}O_4]$ tetrahedra. Uni- and bivalent M^{n+} cations occupy the interstitial positions by $[M^{m+}O_4]$ tetrahedra as ion-compensators of positive charge. Thus, a silica-water-trace element defect in quartz is tripartite. Its left part is acidic. It is composed of two $[SiO_3 \square]$ tetrahedra with a negative charge deficit. The right part consists of two $[M^{m+}O_4]$ tetrahedra. Because M^{m+} is most often M^{3+} (Al^{3+}, Fe^{3+}, etc.), the right part has a positive charge deficit, and is therefore basic. A tetrahedral (_O — $2H^+$) or dipole (H^+ — OH^-) water molecule is incorporated as the shortest Ox — Red bridge in the central part of such a complex. Li, Na, K, Au, Ag, Fe^{2+} and other uni- and bivalent elements enter the interstices by $[M^{m+}O_4]$ tetrahedra for compensating positive charge deficiencies. Weak donor-acceptor and hydrogen bonds formed by the water molecule with the left and right parts of the complex provide its integrity. As this unit is composed of a central H_2O molecule coordinated by positively and negatively charged radicals, it was termed an aqua-complex.

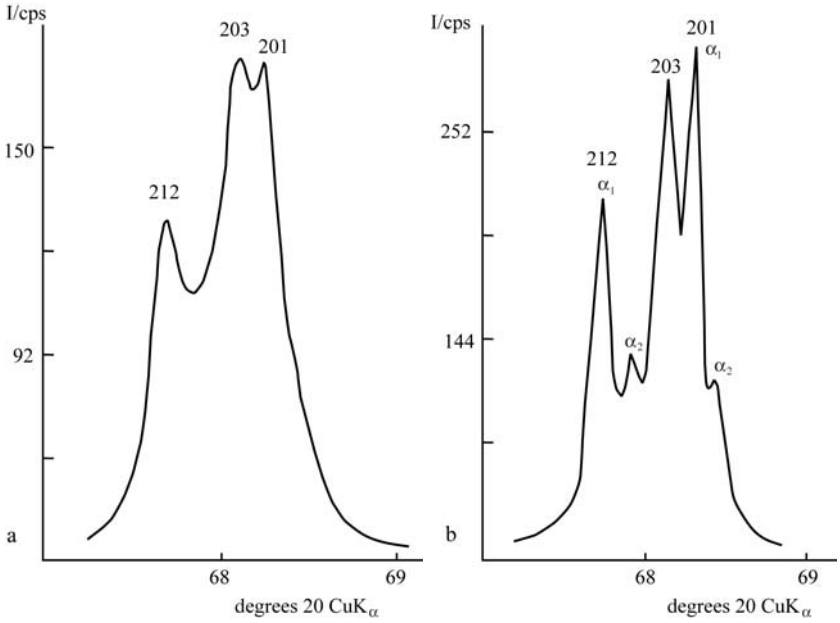

Figure 8. Fragments of X-ray powder diffraction patterns of Q1 (a) and Q2 (b).

Discussion of the aqua-complex

Crystallochemistry

Figure12b shows an aqua-complex built into the structure of α-quartz. This lattice defect is constructed when one of the oxygen bridges between silicons becomes a special oxygen O` that belongs to an H_2O molecule on one side and occupies a regular position in the SiO_4 framework on the other. It therefore may be considered as a bridge oxygen. The outer electron density of this oxygen is shared among two hydrogens and two silicons, therefore its bonds with silicons are donor-acceptor, i.e. electron-unsaturated. Hydrogens of the water molecule located at the edges of the

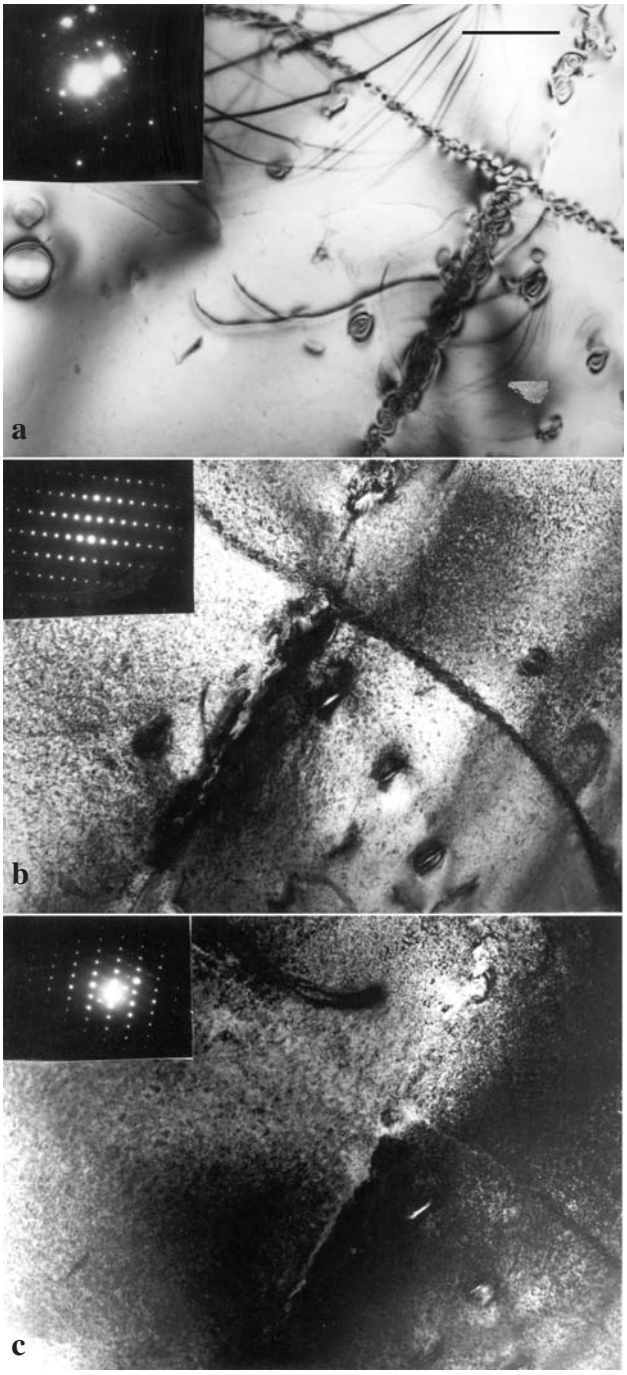

Figure 9. Behaviour of vein quartz (Cu-Mo mineralization) under electron beam: a, b, c refer to 0, 5, 7 minutes of electron irradiation, respectively (scale bar is 1 μm).

[SiO_4] tetrahedra form hydrogen bonds with the oxygens of the neighbouring [$M^{m+}O_4$] tetrahedra. Weak donor--acceptor and hydrogen bonds between the water molecule and the nearest [SiO_4] and [$M^{m+}O_4$] tetrahedra, comprise the three-dimensional continuum of the quartz crystal lattice. In placing the O of the water molecule into the position of a bridge O of the silica lattice (O`), we obtain a structure of intercalating [SiO_4] — [H_2O] tetrahedra (Fig. 12c). This pattern of water incorporation in the [SiO_4] framework was described by Bernal and Fowler (1933) (Fig. 12d), based on the close similarity between the structures of quartz and water. Both are tetrahedra of [SiO_4] and [$\bar{}$ O — $2H^+$] bound to one another by their corners.

Figure 12b necessitates two remarks. First, this sketch ignores the real geometrical relations of the lattice at the site of such a complex defect. Lattice parameters here deviate from those for ideal quartz because of $M^{m+} \rightarrow Si^{4+}$ replacement, the incorporation of M^{n+} into the interstices, and the hydrolysis of Si — O — Si bonds. Such lattice distortions allow H_2O molecules to fit well into the SiO_4-framework. The second remark relates to the location of hydrogens at the O` — O edges of the neighbouring [$SiO_4$] tetrahedra. The length of this edge in a regular quartz structure is 2.65 Å, whereas the O` — H length is 0.9568 Å. It is anticipated that in all hydrogen bonds (O ····· H ····· O) the proton is located in the potential field with two minima (O·····H···H`····· O) (Sienko et al.1968). This situation is shown in Fig.12b by arrows. When $H^+$ is in the nearest O` position, this oxygen has to be taken as the oxygen of a water molecule. When H^+ is at the second minimum (depending on the character of the cation M^{m+} in the neighbouring [$M^{m+}O_4$] tetrahedron), the nearest oxygen of another tetrahedron becomes O`, i.e. the oxygen that belongs simultaneously to a $H_2O$ molecule and the $SiO_4$-lattice. Therefore, in a nonequilibrium medium a particular O` jumps over specific sites in the crystal lattice (Fig. 12b, dotted lines). Every such jump forms a vacancy in the crystal lattice that stimulates the jumping of other chemical bonds. This process is accompanied by the migration of trace elements through the silica network. Thus, as soon as a mineral system becomes unstable, the silica-water-impurity defects are no longer static lattice imperfections; migrating throughout the lattice, they impart a dynamic state to the actual quartz structure.

Aqua-complex in relation to available data on H_2O and trace elements in quartz

At present, there are no direct methods for imaging the aqua-complex in quartz lattices. The only way to prove its existence is to demonstrate that it is consistent with the data on water and trace elements in quartz. Additional support will be obtained if the aqua-complex can account for the peculiarities of quartz and other silica modifications. The key feature of our model is putting the oxygen of a water molecule into the position of bridge oxygen of the SiO_4 – framework. This kind of replacement explains various H-defects: (1) the OH-defect (hydrolysis of Si — OH – HO — Si bonds) responsible for sharp the bands in the 3000–3600 cm^{-1}range (Kats 1962); (2) molecular "water" responsible for the combination band $\nu_{OH} + \delta_{H2O}$ at about 5200 cm^{-1} (Brunner et al. 1961, Langer and Flörke 1974a, b); (3) silanol-group "water" Si — OH, responsible for the combination band $\nu_{OH} + \delta_{Si-OH}$ at 4500 cm^{-1} (Scholze 1960). It also explains the lower symmetry of the proper SiO_4-lattice because of H_2O incorporation (Scholze 1959a, b).

The combination of H-species and trace elements within the same defect has been confirmed by numerous data obtained by IRS (Brunner et al.1961, Langer and

Flörke 1974a, b), atomic or emission spectroscopy (Flörke et al.1982), and, in later works, by cathodoluminescence (Perny et al. 1992, Muller et al. 2003). There is much evidence in the literature on the $\sum M^{n+} \cong \sum M^{m+}$ balance among the uni-, bi-, and multivalent cations of trace elements (Bambauer 1961, Bambauer et al 1961, Chakraborty and Lehman 1976, Rovetta et al. 1989, Flörke et al. 1982, Pankrath and Flörke 1989a, b). The most convincing argument for such a balance was offered by Flörke et al. (1982), who studied cryptocrystalline quartz and agates: $\sum$ at % (½ Ca + ½ Mg + Na + K + Li) correlates positively with $\sum$ at % (Al^{3+} + Fe^{3+}). Kats (1962) also introduced H into the sum of alkali ions.

Transparent quartz annealed at temperatures above 500 °C becomes milky, while the band at 5 200 cm^{-1} attributed to H_2O_{mol} arises in its NIR-spectrum. This unambiguously indicates that water is released from the quartz structure. It should be noted that in this process the H-defect transforms from Si — OH to $H_2O_{mol.}$ Quartz amorphization under electron beam shows that the escape of structural water is accompanied by the breaking chemical bonds in the quartz lattice. Figure13a explains the lack of crystalline continuum of the SiO_4 lattice. Part of the incident electron beam, which is inelastically scattered in a crystal sample, becomes trapped by a network of nonelectron-saturated donor-acceptor bonds between silicons and specific O` atoms. As such bonds take an electron, they become electron-saturated, which results in the escape of water from the silica matrix and the clustering of H_2O molecules in bubbles. After water has been released, a net of vacancies forms in the SiO_4-lattice (Fig. 13a). On heating, they begin to rearrange themselves. This ordering depends on the regime of thermal treatment. Vacancies are annihilated upon quenching, producing again the three-dimensional continuum of a crystal lattice (Fig. 13b). Such quartz samples do not amorphize under the electron beam (Fig. 4a). In samples cooled at a slow rate (annealing), the vacancies form dislocation ensembles associated with clusters of trace elements (Fig. 4b). Figure 13c illustrates a mechanism by which dislocations are generated. A row of broken chemical bonds, i.e. a dislocation core, forms in the SiO_4 lattice as a result of ordering the vacancies. The behaviour of trace elements during the quartz heating resembles that of vacancies. A difference is that interstitial cations M^{n+} leave their structural positions, migrate and form clusters almost as easily as the vacancies do, whereas the mobility of M^{m+} cations through the lattice is hampered by bonding within oxygen tetrahedra. Hence, their ordering on heating results in the formation of coherent inclusions like those present in the quartz from pegmatites (Figs 2c, 3). These inclusions may have compositions close to acmite $NaFeSi_2O_6$ (Morrison-Smith et al. 1976), β-eucryptite $LiAlSiO_4$, β-spodumene $LiAlSi_2O_6$ (Brunner et al. 1961), and structures with lattice parameters close to those of quartz. The scheme (Fig. 12a) shows that these phases can easily appear when the aqua-complexes are agglomerated under their dehydration (defects 1, 3 in Fig. 2c). The aqua-complex explains the uncertainties in identification of lobe-contrast defects. Depending on time of electron irradiation and the character of M^{n+}, M^{m+} cations, a cluster of unordered aqua-complexes (gel defect) may produce tiny water bubbles, clusters of trace elements, generate dislocations and, finally, yield a coherent solid inclusion.

The dynamic behaviour of water-impurity defects under nonequilibrium conditions in mineral systems (Fig. 12b, dotted lines) explains the well-known phenomenon of hydrolytic weakening described first by Griggs and Blacic (1965) and later analyzed in detail by Kronenberg (1994). The jumping of hydrogen bonds, followed by the ordering of vacancies, confirms the possibility of $4H^+ \rightarrow$ Si replacement, which is a hydrogarnet defect predicted in several works (Purton et al. 1992, Lin et al. 1994, Mc Connell et al. 1995).

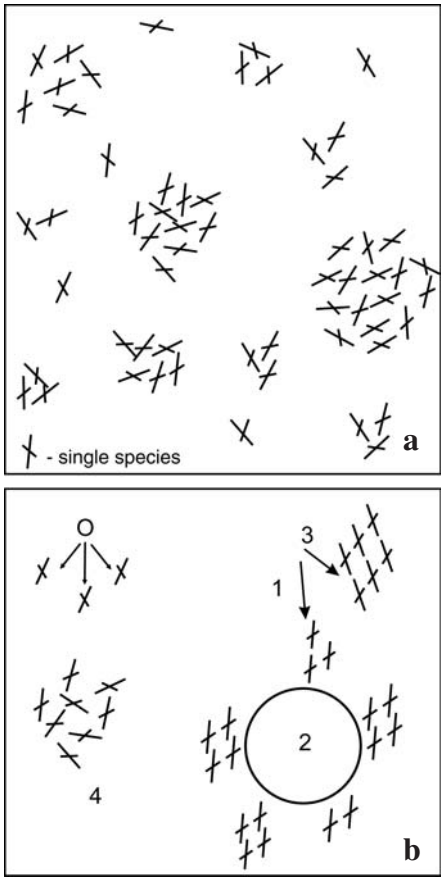

Figure 10. Distribution scheme of silica-water-trace element species in quartz matrix: a – single water-trace element defects and associations of disordered species (gel-defects) in quartz matrix. b – single species (o), their ordered combinations (coherent inclusions – 1,3) associated with gas-liquid bubbles and aggregates of disordered $[SiO_4] - H_2O - M^{n+}M^{3+}$ species (gel-defects) in quartz from pegmatites.

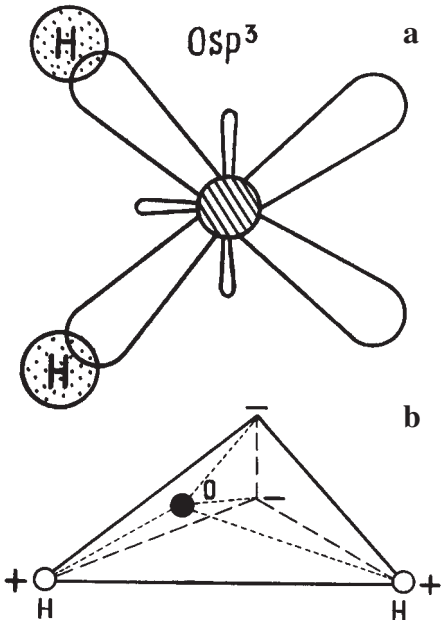

Figure 11. Configuration of water molecules:
a – electron structure, b – representation as charged tetrahedron.

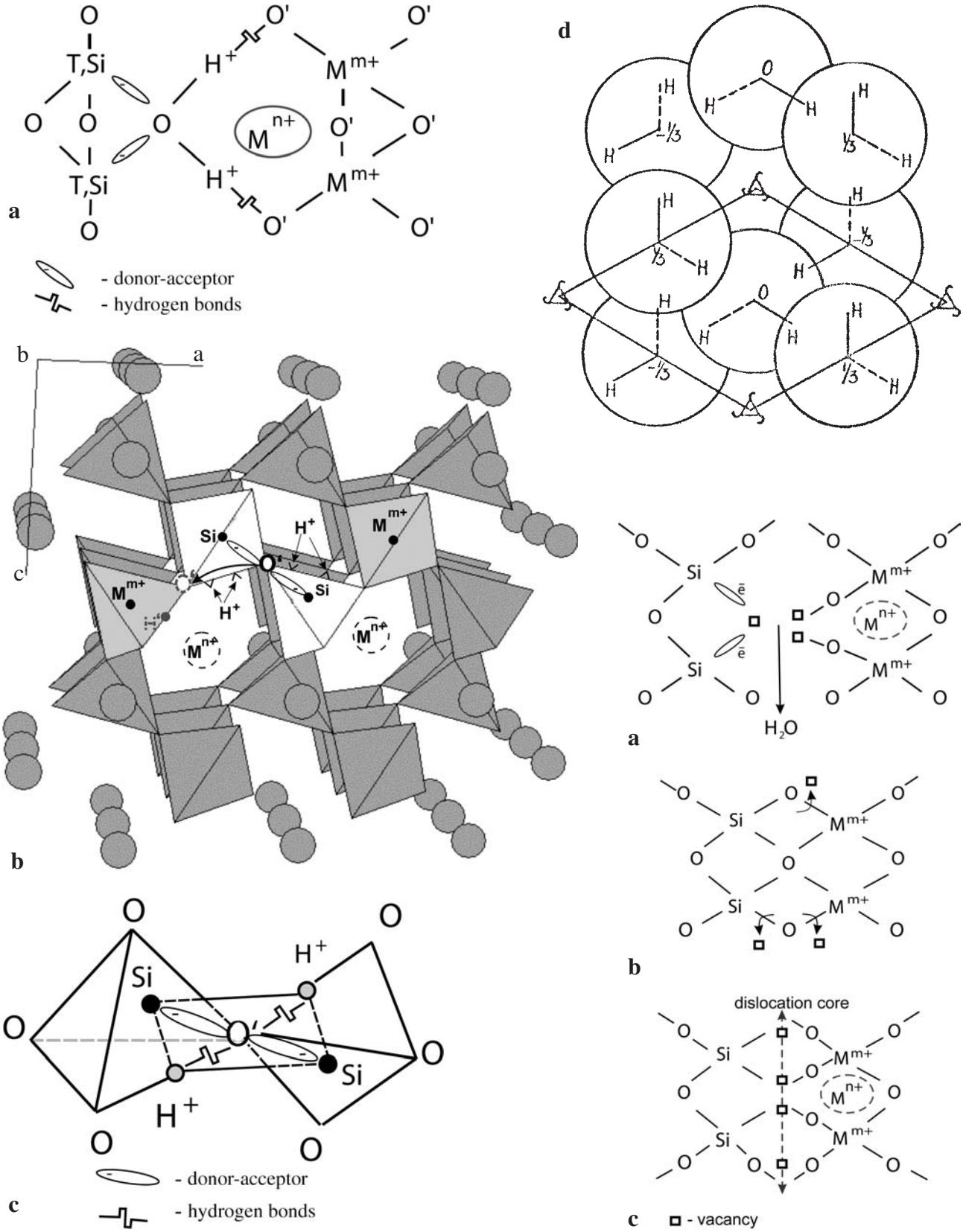

Figure 12. Silica-water-trace element species (aqua-complex) in quartz:
a – scheme of defect: T is tetravalent cation (C, Ti, Sn, etc.), M^{n+} is a uni- and bivalent cation (Li, Na, K, Au, Fe^{2+}, etc.), M^{m+} is a multivalent cation (Al, Fe, P, As, Mo, W, etc.), O` is O and other volatiles (S, Cl, F).
b – incorporation of aqua-complex into quartz SiO_4-framework.
c – intercalated structure of $[SiO_4]$ – $[H_2O]$ tetrahedra.
d – "quartz"-water structure (Bernal and Fowler 1933).

Figure 13. Rearrangements in quartz structure with incorporated aqua-complexes:
a – disintegration of crystalline quartz (amorphization) under electron irradiation.
b – reconstruction of lattice on heating (Fig. 4a).
c – formation of dislocations in annealed sample (Fig. 4b).

Various silica forms in the context of aqua-complex

TEM data show that, depending on its genesis (temperature of crystallization), quartz contains more or less agglomerated aqua-complexes. They are trapped during crystal growth and look like submicrometre- (lobe-contrast, Fig. 2a) and micrometre-scale (Fig. 2e) gel-defects. The aqua-complexes within such inhomogeneities are arbitrarily oriented relative to one another (Fig.10a), reflecting their true state in the mineral-forming medium. It seems that this situation is responsible for the great variety of silica forms in nature. A silica structure composed of regularly packed aqua-complex agglomerations is observed in opal. As the aqua-complex agglomerations are dehydrated, they yield a series of cryptocrystalline silica phases like agates and chalcedonies. The total disintegration at high temperatures of the $[2SiO_3 - H_2O - M^{n+}2M^{m+}O`_4]$ species in the mineral-forming medium produces $SiO_2$ (quartz), which is the left part of the aqua-complex, water as the central part, and $M^{n+}$, $M^{m+}O`_4$ as the right part. Water manifests itself in hydrothermal-metasomatic activity, M^{n+} yields native mineralization (for example gold), and $M^{m+}O`_4$ forms oxides, sulphides, and other salts. Crystallizing quartz traps individual aqua-complexes and their disordered (gel-like) associations. Individual aqua-complexes with a wide range of elements replacing M^{n+}, M^{m+} positions are responsible for the various colour modifications of quartz, such as citrine, amethyst, and smoky quartz.

A special case is vein quartz associated with ore mineralization. Its generations are connected with complex structural and chemical rearrangements of the silica matrix saturated with aqua-complex defects. Our data (Stenina et al. 1988, Stenina et al. 1993, Stenina et al. 2000) show that this process within the silica continuum is responsible for Cu-Mo, and Au-sulphide mineralization in vein deposits.

Conclusions

A combined defect $[2SiO_3 \square - OH_2 - M^{n+}2M^{m+}O`_4]$ called an aqua-complex fits all forms of water and trace element occurrences in the silica matrix. The aqua-complexes, as the units of a mineral-forming medium, are trapped in quartz on crystallization. This defect is metastable in the SiO_4 framework and is, therefore, characterized by dynamic behaviour in a non-equilibrium mineral system. Accordingly, H (H_2O), interstitial M^{n+}, and tetrahedrally coordinated M^{m+} foreign cations migrate through the quartz lattice, which rearranges itself in the process. Such properties of the aqua-complex as a lattice defect in quartz explain why it has long escaped detection by numerous analytical methods.

Acknowledgements. The author is profoundly grateful to Prof. L. M. Plyasova, Prof. A. K. Gutakovskii, Dr. D. B. Karimova, Dr. V. N. Korolyuk, and T. P. Borozdina for assistance at various stages of this investigation.

References

Aines R. D., Kirby S. H., Rossman G. R. (1984): Hydrogen speciation in synthetic quartz. Phys. Chem. Mineral. 11, 204–212.

Aines R. D., Rossman G. R. (1984): Water in minerals? A peak in the Infrared. J. Geophys. Res. 89, 4059–4071.

Ashby M. F., Brown L. M. (1963a): Diffraction contrast from spherically symmetrical coherency strains. Philos. Mag. 8, 1063–1103.

Ashby M. F., Brown L. M. (1963b): On the diffraction contrast from inclusions. Philos. Mag. 8, 1649–1676.

Baker C. (1970): The effect of heat treatment and nitrogen addition on the critical current density of a worked Niobium, 44 wt% Titanium superconducting alloy. J. Mater. Sci. 5, 40–52.

Balakirev V. G., Kievlenko E. Y., Nikol'skaya L. V., Samoilovich M. I., Hadzhi V. E., Tsinober L. I. (1979): Mineralogy and crystallophysics of the gem varieties of silica. Nedra, Moscow. (in Russian)

Balitskii V. S., Balitskaya O. V. (1985): Bicoloures amethyste-citrine quartz and conditions of its formation. ZVMO 114, 664–676.

Bambauer H. U. (1961): Spurenelementgehalte und Farbzentren in Quarzen aus Zerrklüften der Schweizer Alpen. Schweiz. Mineral. Petrogr. Mitt. 41, 335–369.

Bambauer H. U., Brunner G. O., Laves F. (1961): Beobachtungen ueber Lamellenbau in Bergkristallen. Z. Kristall. 116, 176–181.

Bambauer H. U., Brunner G. O., Laves F. (1962): Wasserstoff-Gehalte in Quarzen aus Zerrklüften der Schweizer Alpen und die Deutung ihrer regionalen Abhängigkeit. Schweiz. Mineral. Petrogr. Mitt. 42, 221–236.

Bazarov L. S., Stenina N. G. (1978): The influence of heat treatment on the defect structure of natural quartz. Dokl. Akad. Nauk USSR 243, 1261–1264.

Bernal J. D., Fowler R. H. (1933): A theory of water and ionic solution, with particular reference to hydrogen and hydroxyl ions. J. Chem. Phys. 1, 515–548.

Brunner G. O., Wondratschek H., Laves F. (1961): Ultrarotuntersuchungen übr der Einbau von H in natürlichen Quarz. Z. Elektrochem. 65, 735–750.

Chakraborty D., Lehman G. (1976): Distribution of OH in synthetic and natural quartz crystals. J. Solid State Chem. 17, 305–311.

Cordier P., Doukhan J. C. (1989): Water solubility in quartz and its influence on ductility. Eur. J. Mineral. 1, 221–237.

Cordier P., Doukhan J. C. (1991): Water speciation in quartz: a near infrared study. Am. Miner. 76, 361–369.

Flörke O. W., Köhler-Herbertz B., Langer K., Tönges I. (1982): Water in microcrystalline quartz of volcanic origin: agates. Contrib. Mineral. Petrol. 80, 324–333.

Frondel C. (1982): Structural hydroxyl in chalcedony (type B quartz). Am. Miner. 67, 1248–1257.

Graetsch H., Flörke O. W., Miehe G. (1985): The nature of water in chalcedony and opal-C from Brazilian agate geodes. Phys. Chem. Miner. 12, 300–306.

Griggs D. T., Blacic J. D. (1965): Quartz: anomalous weakness of synthetic crystals. Science 147, 292–295.

Heaney P. J. (1993): A proposal mechanism for the growth of chalcedony. Contrib. Mineral. Petrol. 115, 66–74.

Heggie M. I. (1992): A molecular water pump in quartz dislocations. Nature 355, 337–339.

Heydenreich J. (1969): Transmission electron microscopic investigations of thin monocrystalline alkali halide foils. Roumaine de Physique 14, 1253–1265.

Hirsch P. B., Howie A., Nicholson R. B., Pashley D. O. W., Whelan M. J. (1968): Electron microscopy of thin crystals. Mir, Moscow. (in Russian)

Hopkinson L., Roberts S., Herrington R., Wilkinson J. (1999): The nature of crystalline silica from the TAG submarine hydrothermal mound, 26°N Mid Atlantic Ridge. Contrib. Mineral. Petrol. 137, 342–350.

Kats A. (1962): Hydrogen in alpha-quartz. Philips Res. Rep. 17, 133–279.

Kekulawala K. R. S. S., Paterson M. S., Boland J. N. (1978): Hydrolytic weakening in quartz. Tectonophysics 46, T1–T6.

Kronenberg A. K. (1994): Hydrogen speciation and chemical weakening of quartz. Rev. Mineral. 29, 123–176.

Langer K., Flörke O. W. (1974a): Wasser in Opal und Hyalite. Fortschr. Miner. 51, 80–82.

Langer K., Flörke O. W. (1974b): Near infrared absorption spectra

(4000–9000 cm^{-1}) of opals and the role of "water" in these $SiO_2 – nH_2O$ minerals. Fortschr. Miner. 52, 17–51.

Laudise R. A., Ballman A. A., King J. C. (1965): Impurity content of synthetic quartz and its effect upon mechanical q. J. Phys. Chem. Solids 26, 1305–1308.

Lin J. S., Payne M. C., Heine V., McConnell J. D. C. (1994): Ab initio calculations on $(OH)_4$ defects in α-quartz. Phys. Chem. Miner. 21, 150–155.

McConnell J. D. C., Lin J. C., Heine V. (1995): The solubility of $[4H]_{Si}$ defects in α-quartz and their role in the formation of molecular water and related weakening on heating. Phys. Chem. Miner. 22, 357–366.

McLaren A. C., Cook R. F., Hyde S. T., Tobin R. C. (1983): The mechanisms of the formation and growth of water bubbles and associated dislocation loops in synthetic quartz. Phys. Chem. Miner. 9, 79–94.

McLaren A. C., Fitz Gerald J. D., Gerretsen J. (1989): Dislocation nucleation and multiplication in synthetic quartz: relevance to water weakening. Phys. Chem. Miner. 16, 465–482.

McLaren A. C., Phakey P. P. (1965): A transmission electron microscope study of amethyst and citrine. Aust. J. Phys. 18, 135–141.

McLaren A. C., Phakey P. P. (1966): Transmission electron microscope study of bubbles and dislocations in amethyst and citrine quartz. Aust. J. Phys. 19, 19–24.

Morrison-Smith D. J., Paterson M. S., Hobbs B. E. (1976): An electron microscope study of plastic deformation in single crystals of synthetic quartz. Tectonophysics 33, 43–79.

Müller A., Wiedenbeck M., Van den Kerkhof A. M., Kronz A., Simon K. (2003): Trace elements in quartz – a combined electron microprobe, secondary ion mass spectrometry, laser ablation ICP-MS, and cathodoliminescence study. Eur. J. Mineral. 15, 747–763.

Nuttal R. D. Weil J. A. (1980): Two hydrogenic trapped-hole species in α-quartz. Solid State Commun. 33, 99–102 .

Pankrath R., Flörke O. W. (1989a): Einfluss von Natrium und Lithium ionen auf der Al, Si-Austauschkinetik in Tief- und Hoch- Quarz und Berechnung von Diffusionskoeffizienten für Al. Z. Kristall. 186, 219–220.

Pankrath R., Flörke O. W. (1989b): Polarisierte IR-Einkristallspektren synthetischer Rauchquarze. Z. Kristall. 186, 220–222.

Perny B., Eberhardt P., Ramseyer K., Mullis J., Pankrath R. (1992): Microdistribution of Al, Li and Na in α-quartz: Possible causes and correlation with short-lived cathodoluminescence. Am. Miner. 77, 534-544.

Purton J., Jones R., Heggie M., Öberg S., Catlow C. R. A. (1992): LDF pseudopotential calculations of the α-quartz structure and hydrogarnet defect. Phys. Chem. Miner. 18, 389–392.

Rovetta M. R., Blacic J. D., Hervig R. L., Holloway J. R. (1989): An experimental study of hydroxyl in quartz using infrared spectroscopy and ion microprobe techniques. J. Geophys. Res. 94, 5840–5850.

Scholze H. (1959a): Der Einbau des Wassers in Glüsern. I Der Einfluss des in Gläsgelësten Wassers auf das Ultrarot-Spektrum und die quantitative ultrarotspektroskopische Bestimmung des Wassers in Gläsern. Glastechn. Ber. 32, 81–88.

Scholze H. (1959b): Der Einbau des Wassers un Gläsern. II UR-Messungen in Silikat glaesern mit systematisch varierter Zusammensetzung und Deutung der OH-Banden in Silikatgläsern. Glastechn. Ber. 32, 142–152.

Scholze H. (1960): Zur Frage der Unterscheidung zwischen H_2O Moleküln und OH-Gruppen in Gläsern und Mineralen. Naturwissenschaften 10, 226–227.

Sienko M. J., Plane R. A., Hester R. E. (1968): Structural inorganic chemistry. Mir, Moscow. (in Russian)

Stenina N. G. (1987): On the forms of water incorporation into crystalline quartz. Mineral. Mag. 9, 58–69. (in Russian)

Stenina N. G., Bazarov L. S., Scherbakova M. Y., Mashkovtsev R. I. (1984): Structural state and diffusion of impurities in natural quartz of different genesis. Phys. Chem. Miner. 10, 180–186.

Stenina N. G., Distanova A. N., Berezin Y. A. (1993): Au-Fe associations in silicate phases as evidence of gold transportation via aqua-complexes. In: Fenoll Hach-Ali P. et al. (eds) Current Research in Geology Applied to Ore Deposits. University of Granada, Granada, Spain, pp. 567–570.

Stenina N. G., Gubareva D. B., Gutakovskii A. K., Plyasova L. M. (2000): Crystallochemical peculiarities of vein quartz of the Sarala deposit (Kuznetskii Alatau, Russia) as indicator of productivity of gold mineralization. Geol. Ore Depos. 42, 53–62. (in Russian)

Stenina N. G., Sotnikov V. I., Korolyuk V. N., Kovaleva L. T. (1988): Microstructural peculiarities of hydrothermal vein quartz as indicator of its ore-bearing capacity. Geochimiya 5, 641–653.

Weil J. A. (1984): A review of electron spin specroscopy and its application to the study of paramagnetic defects in crystalline quartz. Phys. Chem. Miner. 10, 149–165.

Yurgenson G. A. (2003): Typomorphism and ore formations. Nauka, Novosibirsk. (in Russian)